

# High-pressure studies on fluorine substituted 2,5-di(phenyl)-1,3,4-oxadiazoles

Ingo Orgzall<sup>a,\*</sup>, Olga Franco<sup>b,1</sup>, Günter Reck<sup>c</sup>, Burkhard Schulz<sup>b</sup>

<sup>a</sup>Institut für Dünnschichttechnologie und Mikrosensorik e. V. Kantstraße 55, D-14513 Teltow, Germany

<sup>b</sup>Universität Potsdam, Institut für Physik, Am Neuen Palais 10, D-14469 Potsdam, Germany

<sup>c</sup>Bundesanstalt für Materialforschung und Prüfung (BAM), Richard-Willstätter-Straße 11, D-12489 Berlin, Germany

Received 6 January 2005; revised 10 March 2005; accepted 11 March 2005

Available online 31 May 2005

## Abstract

Results are presented from structural and high-pressure investigations on four differently but symmetrically fluorine substituted 2,5-di(phenyl)-1,3,4-oxadiazoles. The substitution pattern includes the *para*-, *meta*-, or *ortho*-substitution and the fully fluorinated 2,5-bis(pentafluorophenyl)-1,3,4-oxadiazole. The crystal structure depends on the molecular structure and results in a different high-pressure behavior. Parameters for the Murnaghan equation of state (EOS) are determined for every compound and the anisotropic pressure response of the crystal lattice is discussed. Although the EOS parameters, bulk modulus  $K_0$  and its pressure derivative  $K'_0$  are of the same order of magnitude for all four compounds, the anisotropy of strain is noticeably different.

© 2005 Elsevier B.V. All rights reserved.

**Keywords:** Oxadiazole; Molecular crystal; Crystal structure; High pressure; Equation of state

## 1. Introduction—high pressure as a tool

High-pressure investigations belong to indispensable techniques in many fields of basic as well as applied sciences, ranging from solid state physics, chemistry, geophysics and geology up to materials science and even biochemical and biological problems [1–4].

Although high-pressure studies provide a unique insight into the complex relations between structure and properties due to the tuning of the intermolecular interactions by variation of the distances between the individual building units, the application in the field of organic solids is still emerging. Some reviews summarizing the developments and achievements in this field are found in [4–8]. Such studies have even a practical impact and it is only shortly

mentioned here that high-pressure investigations like the determination of an equation of state (EOS) or the study of possible phase transitions are particularly important for the pharmaceutical industry [7,9,10]. Besides volume changes, phase transitions may also occur during pressure application possibly leading to a different polymorph that exhibits new properties.

Principally, most organic crystals show high compressibility and strong anisotropy. Observing the high-pressure behavior of organic molecular crystals the question emerges, whether there exist some general rules rather independent on the individual molecular structure or if this individual structure and therefore the specific intermolecular interactions determines the pressure response of the solid. Such influences result for instance from the structure of the aromatic system, i.e. from the number of rings and their mutual arrangement. This determines the conformation of the molecule, its planarity and thus a possible conjugation. Further points that deserve some attention are differences in polarity (dipole moment) or shape anisotropy. Distinctions in the supramolecular arrangement like the occurrence of stacks or layers in the crystal structure may also influence the high-pressure behavior. Additionally, specific molecular structures or functional groups could cause steric influences and hindrances or could favor

\* Corresponding author. Tel.: +49 3328 3346 0; fax: +49 3328 3346 10.  
E-mail addresses: [orgzall@rz.uni-potsdam.de](mailto:orgzall@rz.uni-potsdam.de) (I. Orgzall), [franco@rz.uni-potsdam.de](mailto:franco@rz.uni-potsdam.de) (O. Franco), [guenter.reck@bam.de](mailto:guenter.reck@bam.de) (G. Reck), [buschu@rz.uni-potsdam.de](mailto:buschu@rz.uni-potsdam.de) (B. Schulz).

<sup>1</sup> Present address: Departamento de Química Física I, Facultad de Ciencias Químicas, Universidad Complutense, Ciudad Universitaria, E-28040 Madrid, Spain.

the formation of hydrogen bonds. The anisotropic compression due to the molecular arrangement provides insights into the action of the different forces constituting the organic molecular crystal as for instance  $\pi$ - $\pi$ , van der Waals, or hydrogen bond interactions.

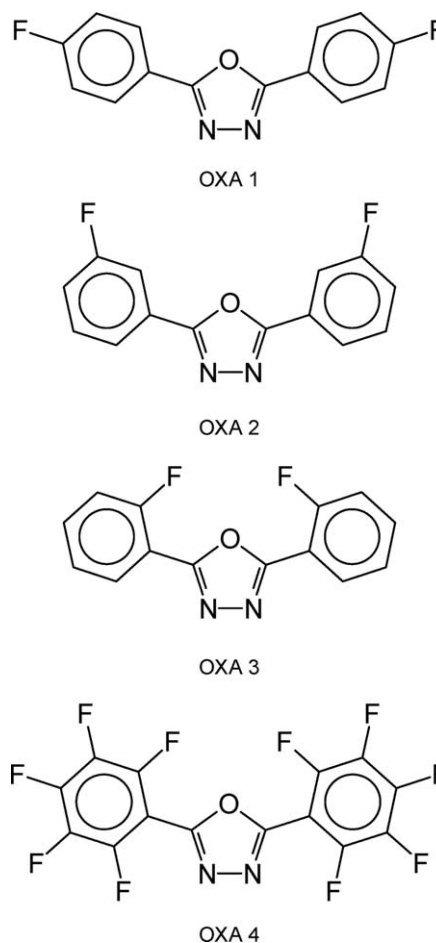
Many investigations always include a group of similar or related compounds that differ only in their substitutional scheme to deduce some generalities and trends and to relate them to the specific chemical structure (see, for instance [11–14] for studies on biphenyl, oligophenyls, or *para*-hexaphenyl, respectively, and [15–17] for anthracene and disubstituted anthracene derivatives or [18] for further compounds). Investigating the crystal structures of some drugs under compression up to 4 GPa either by single crystal or by powder diffraction techniques usually high compressibilities resulted. Especially these studies discuss the strong anisotropic lattice response to pressure application, i.e. the lattice strain in relation to the molecular conformation, the crystal packing, the corresponding intermolecular interactions, or specific intermolecular bonds [6–8,19].

In the following, a comprehensive experimental study will be outlined summarizing results of structural studies and investigations of the compression behavior of differently substituted 2,5-di(phenyl)-1,3,4-oxadiazoles with fluorine as substituent. The aim is to contribute to the question whether there exist some similarities or general trends within this class of compounds with changing substitution scheme (*ortho*-, *meta*-, *para*-, or perfluorinated compounds) or even in comparison with other organic molecules based on similar molecular or supramolecular structures and specifically with other di(phenyl)-oxadiazoles [20–22]. The results could also be compared to high-pressure studies of different halogenated molecules like fluorinated or chlorinated phenols [23] or chlorinated ethane [24]. Although the molecular structures are somewhat different compared to the compounds investigated here the pressure effects are quite similar as the compression behavior is considerably determined by the different intermolecular interactions involving the halogen atoms like hydrogen bonds or halogen–halogen interactions. Specific attention is paid to the structural modification introduced by the changing substituent's position and the resulting consequences for the bulk high-pressure behavior or the compression anisotropy.

## 2. Experimental setup

### 2.1. Sample preparation

The investigated fluorine containing 2,5-di(phenyl)-1,3,4-oxadiazole compounds were synthesized by direct condensation of fluorobenzoic acid with hydrazine hydrate in polyphosphoric acid. The fluorobenzoic acid and hydrazine hydrate were stirred in polyphosphoric acid



Scheme 1.

(84.6%  $P_2O_5$ ) at 180 °C for 2 h. After cooling, the clear solutions were poured into water, filtered and the products were dried in vacuum. The products were three times recrystallized from ethanol or hexane. Melting points: *para*-substitution, 2,5-bis-(4-fluorophenyl)-1,3,4-oxadiazole (OXA 1): 201 °C (lit. 213 °C [25]) (for the molecular structure cf. Scheme 1), *meta*-substitution, 2,5-bis-(3-fluorophenyl)-1,3,4-oxadiazole (OXA 2): 134 °C, *ortho*-substitution, 2,5-bis-(2-fluorophenyl)-1,3,4-oxadiazole (OXA 3): 116 °C (commercially available, Lancaster, 112–114 °C), 2,5-bis-(pentafluorophenyl)-1,3,4-oxadiazole (OXA 4): 151–155 °C (156–158 °C [26,27]).

### 2.2. Crystal structure determination and results

The crystal structures have been determined by single crystal structure analysis. The X-ray data were collected on a Bruker AXS SMART/CCD diffractometer. The structures were solved by direct methods and refined by full-matrix least-squares calculations using SHELX-97 [28]. For OXA 1 and OXA 3 all hydrogen atoms were located by difference Fourier synthesis. The crystals of OXA 2 were twinned. This was taken into account in the structure refinement using the twin matrix (1 0 0/0 1 0/0 0 -1). Hydrogen atom

positions of OXA 2 were calculated corresponding to their geometrical conditions and refined using the riding model. The molecule of OXA 3 contains a two-fold axis coinciding with that of the space group  $C2/c$ . Therefore, only the atomic coordinates of half of the molecule must be determined. The crystallographic data have been deposited at the Cambridge Crystallographic Data Center as supplementary publication Nos. CCDC 255251 for OXA 1, CCDC 255252 for OXA 2, CCDC 255253 for OXA 3, and CCDC 255254 for OXA 4. These data can be obtained free of charge via [www.ccdc.cam.ac.uk/conts/retrieving.html](http://www.ccdc.cam.ac.uk/conts/retrieving.html).

### 2.3. High-pressure investigations

All structure investigations under high pressure were carried out in the multi-anvil press MAX-80 [29] using synchrotron radiation at HASYLAB, DESY Hamburg. The sample container, an epoxy cube, serving as pressure transmitting medium, is filled with the ground sample and NaCl as pressure standard in separate layers and sealed by a pyrophyllite disk.

The diffractograms are recorded by an energy dispersive detector with multi-channel analyzer. Some disadvantages have to be considered: texture effects due to the powder technique, a generally lower resolution compared to angle resolved methods, the occurrence of additional diffraction lines due to the detector material (escape peaks) or to the surrounding epoxy material [30]. This was taken into account during the evaluation of the diffractograms.

The pressure is determined in situ applying the well-known equation of state for NaCl, i.e. the Decker equation [31]. The corrections to that scale introduced by the work of Brown [32] remain small in the investigated pressure region. Two diffractograms are recorded at every pressure step, one of the sample and one of NaCl for pressure determination. Slight gradients of around 0.1 GPa within the sample due to non-hydrostatic effects cannot be ruled out due to the comparatively large volume of the pressure cell.

For the subsequent evaluation of the diffractograms and the determination of the lattice parameters the program Powder Cell 2.3 [33] is applied. The experimental patterns were fitted using the structure data for the ambient pressure structure that resulted from single crystal investigations as starting point. The special recourse procedure offered by the program enables this evaluation independently on texture influences upon the intensity of the peaks. Here, the intensity of every peak is treated separately. The shape of the crystals always introduced texture effects although all samples were carefully ground. Sometimes an increasing texture was observed under pressure due to the alignment of the small crystallites. The relative error of the fit procedure to determine the lattice parameters using Powder Cell is estimated to 0.003 for the axis lengths, slightly larger for the monoclinic angle (for clarity error bars are not given for every pressure step in the figures). Of course, the resulting

error also depends on the quality of the experimental energy dispersive pattern and slightly increases with pressure.

This procedure delivers information only about the variation of the lattice parameters but not on the crystal symmetry or the individual atomic positions. A deeper analysis to determine the appropriate molecular conformation is impossible due to the low resolution of the diffractograms and the disturbing influences from the gasketing cube. It is supposed that the crystal symmetry remains always that of the ambient pressure structure. Nevertheless, the resemblance of the diffraction patterns under pressure to that pattern under ambient conditions also in its relative intensities justifies this approach. It was proven that the diffraction pattern is sensitive to larger orientational changes and rotations of the individual molecules as well as to variations of the mutual positions what would change the whole pattern. However, some slight changes of both, molecular conformation and mutual position of the individual molecules cannot fully be ruled out. In general the main structural elements like stack or layer arrangement of the di(phenyl)-1,3,4-oxadiazole compounds should be maintained also under pressure. The evaluation procedure therefore also involves that the conformation of the molecule remains unaltered. This approximation describes well the behavior of aromatic compounds with a partially delocalized  $\pi$  system like the oxadiazoles. This approach is reasonable since it is usually expected that the compression of the intramolecular bond lengths is much smaller compared to that of the intermolecular distances.

## 3. Results and discussion

### 3.1. Crystal structure

Table 1 summarizes the crystallographic data for all investigated compounds OXA1 - OXA4. All structures belong to the monoclinic system but show different packing motifs for the individual compounds.

Fig. 1 shows the ORTEP plots of the molecules of OXA 1, OXA 2, OXA 3, and OXA 4. The mean N–C distance of 1.287(8) Å of all compounds indicates enlarged double bond character between these atoms in the oxadiazole ring. The mean O–C and N–N bonds are 1.364(7) and 1.411(9) Å, respectively, indicating single bonds between the corresponding atoms. In OXA 1, OXA 2, and OXA 3, only one fluorine atom is bound to each phenyl ring. The mean C–F bond amounts to 1.362(9) Å. In OXA 4, all hydrogen atoms are substituted by fluorine atoms. In this compound the C–F distances are significantly shorter than the C–F bonds in OXA 1, OXA 2, and OXA 3. In OXA 4 the mean C–F bond amounts to 1.338(5) Å. Remarkably, in the case of *ortho*- and *meta*-substitution the bond between phenyl ring and fluorine substituent points into the direction of the oxygen atom contrary to symmetric *meta*- and *ortho*-amino

Table 1  
Crystallographic data and structure determination for the investigated compounds OXA1–OXA4 at ambient pressure

	OXA 1	OXA 2	OXA 3	OXA 4
Formula	C <sub>14</sub> H <sub>8</sub> F <sub>2</sub> N <sub>2</sub> O	C <sub>14</sub> H <sub>8</sub> F <sub>2</sub> N <sub>2</sub> O	C <sub>14</sub> H <sub>8</sub> F <sub>2</sub> N <sub>2</sub> O	C <sub>14</sub> F <sub>10</sub> N <sub>2</sub> O
Formula weight	258.22	258.22	258.22	402.16
Temperature (K)	293(2)	293(2)	293(2)	293(2)
Wavelength (Å)	0.71073	0.71073	0.71073	0.71073
Crystal system	Monoclinic	Monoclinic	Monoclinic	Monoclinic
Space group	<i>P</i> 2 <sub>1</sub> / <i>n</i>	<i>P</i> 2 <sub>1</sub> / <i>n</i>	<i>C</i> 2/ <i>c</i>	<i>P</i> 2 <sub>1</sub> / <i>n</i>
Unit cell dimensions	<i>a</i> = 10.44(2) Å <i>b</i> = 11.44(2) Å <i>c</i> = 10.75(2) Å $\beta$ = 116.31(9)°	<i>a</i> = 3.98(2) Å <i>b</i> = 24.24(7) Å <i>c</i> = 12.44 (4) Å $\beta$ = 90.12(6)°	<i>a</i> = 13.864(6) Å <i>b</i> = 12.397(5) Å <i>c</i> = 7.079(3) Å $\beta$ = 110.284(8)°	<i>a</i> = 12.32(2) Å <i>b</i> = 4.701(6) Å <i>c</i> = 23.65(4) Å $\beta$ = 104.96(3)°
Volume (Å <sup>3</sup> )	1151(4)	1199(7)	1141.3(8)	1324(3)
Z, calculated density (g cm <sup>-3</sup> )	4, 1.490	4, 1.430	4, 1.503	4, 2.018
Absorption coefficient (mm <sup>-1</sup> )	0.118	0.114	0.119	0.226
<i>F</i> (000)	528	528	528	784
Crystal size (mm <sup>3</sup> )	0.24 × 0.16 × 0.03	1.00 × 0.06, 0.04	0.65 × 0.22 × 0.18	0.30 × 0.04 × 0.03
Range for data collection (°)	2.26–23.0	1.64–23.0	2.27–25.0	1.71–30.0
Limiting indices	–15 ≤ <i>h</i> ≤ 12 –15 ≤ <i>k</i> ≤ 14 –12 ≤ <i>l</i> ≤ 15	–5 < <i>h</i> < 5 –28 < <i>k</i> < 33 –15 < <i>l</i> < 12	–17 < <i>h</i> < 19 –14 < <i>k</i> < 15 –9 < <i>l</i> < 9	–15 < <i>h</i> < 17 –6 < <i>k</i> < 6 –33 < <i>l</i> < 23
Reflection unique	1602	1674	1005	3571
Refinement method	Full-matrix least-squares on <i>F</i> <sup>2</sup>	Full-matrix least-squares on <i>F</i> <sup>2</sup>	Full-matrix least-squares on <i>F</i> <sup>2</sup>	Full-matrix least-squares on <i>F</i> <sup>2</sup>
Goodness-of-fit on <i>F</i> <sup>2</sup>	1.048	1.101	1.018	0.608
Final <i>R</i> indices	<i>R</i> 1 = 0.076 <i>R</i> 2 = 0.177	<i>R</i> 1 = 0.081 <i>R</i> 2 = 0.177	<i>R</i> 1 = 0.039 <i>R</i> 2 = 0.113	<i>R</i> 1 = 0.038 <i>R</i> 2 = 0.096

substitution or *ortho*-nitro substitution, where the bonds between these groups and the phenyl ring always point into the direction of the nitrogen atoms [34].

The conformation of the molecules can be described by the dihedral angles between the central oxadiazole and the phenyl rings. The angles between the planes as marked in Fig. 1 are given in Table 2. The C–C distances between the oxadiazole and phenyl rings range from 1.451 to 1.474 Å (Table 2). However, no correlations between bond lengths and deviations from coplanarity were recognized. It is interesting to note, that OXA 3 with its *ortho*-substitution shows the largest deviations from planarity (torsion angle 28.9°). These experimental values may be compared to theoretical Cerius<sup>2</sup> calculations of the single molecules given in [35] for OXA 3 and OXA 4. According to these calculations OXA 4 should have the largest torsion angle between oxadiazole and phenyl rings (32.5°) compared to roughly 14° found here, while the OXA 3 molecule should be completely planar (0°).

In the compounds OXA 1, OXA 2, and OXA 3  $\pi$ – $\pi$  electron interactions develop between symmetry related molecules. These interactions are defined by the distance between the ring centroids (DC), the perpendicular distances of the centroids of one ring to the plane of the other (DP) and the intermolecular angle ( $\alpha$ ). The corresponding rings are marked in Fig. 1. The interactions are evaluated using the Platon program [36]. Since this program does not give standard deviations of the parameters, these have to be estimated. The maximum error of the distances is

expected to be smaller than 0.006 Å and that of the angle  $\alpha$  smaller than 0.2°. Table 3 lists these interaction parameters for OXA 1. These  $\pi$ – $\pi$  electron interactions between phenyl and oxadiazole rings of adjacent molecules give rise to the formation of molecular layers in the crystal structure of OXA 1 parallel to the *a*,*c*-plane as depicted in Figs. 2(a) and (b). Additionally, the molecules within a layer are held together by two symmetry independent intermolecular C–H···F hydrogen bonds, namely C10–H···F19<sup>i</sup> (*i*: 1.5 + *x*, –1.5 – *y*, 0.5 + *z*; C–F = 3.32 Å, H–F = 2.38 Å, C–H–F = 142.6°) and C16–H···F18<sup>ii</sup> (*ii*: –1.5 + *x*, –1.5 – *y*, –0.5 + *z*; C–F = 3.44 Å, H–F = 2.44 Å, C–H–F = 154.8°). These and the symmetry related hydrogen bonds form molecular chains within the layers (see Fig. 2(b)).

The numerical values describing the  $\pi$ – $\pi$  electron interactions for OXA 2 are found in Table 4. These and the symmetry related  $\pi$ – $\pi$  electron interactions connect the molecules of OXA 2 forming stacks extended in *a*-direction (see Figs. 3(a) and (b)).

In OXA 3  $\pi$ – $\pi$  or dipole–dipole electron interactions appear only between the central oxadiazole rings. These interactions are the same for all four interactions between Cg1 and Cg1 at (–*x*, –*y*, –*z*), (–*x*, –*y*, 1 – *z*), (*x*, –*y*, –1/2 + *z*), and (*x*, –*y*, 1/2 + *z*), respectively. The corresponding distances are DC = 3.617 Å, DP = 3.482 Å, DP = 3.482 Å, and  $\alpha$  = 0°. These interactions give rise to the formation of stacks extended in *c*-direction. The stacks and the corresponding molecular packing are shown in Figs. 4(a) and (b), respectively.

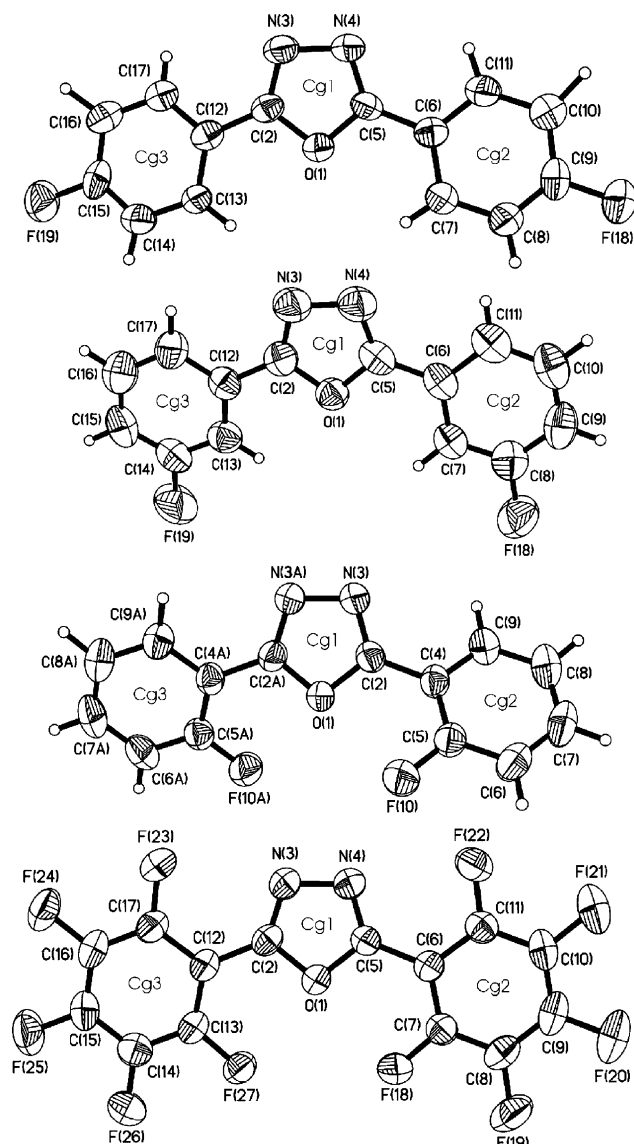


Fig. 1. Molecular structures of OXA 1, OXA 2, OXA 3, and OXA 4, showing 50% probability displacement ellipsoids.

Surprisingly, there are no  $\pi$ – $\pi$  electron interactions in the crystal structure of OXA 4 because the shortest Cg–Cg distances are larger than 4.7 Å. There is no overlap between parallel and likewise oriented molecules. Probably, this is

Table 2  
Dihedral angles (first line) and bond distances (second line) between the different aromatic rings (cf. Fig. 1).

	Cg1–Cg2	Cg1–Cg3	Cg2–Cg3
OXA 1	12.9° 1.451 Å	16.1° 1.451 Å	6.2° –
OXA 2	6.0° 1.474 Å	3.8° 1.467 Å	8.2° –
OXA 3	28.9° 1.458 Å	28.9° 1.458 Å	54.1° –
OXA 4	14.1° 1.465 Å	14.2° 1.462 Å	8.8° –

Table 3  
Parameters for  $\pi$ – $\pi$  interactions in OXA 1

Interactions between	DC (Å)	DP (Å)	DP (Å)	$\alpha$ (°)
Cg1 and Cg2 at ( $-1/2+x, 1/2-y, -1/2+z$ )	3.651	3.537	3.565	3.50
Cg1 and Cg3 at ( $1/2+x, 1/2-y, 1/2+z$ )	3.566	3.438	3.517	7.63
Cg2 and Cg1 at ( $1/2+x, 1/2-y, 1/2+z$ )	3.651	3.565	3.537	3.50
Cg3 and Cg1 at ( $-1/2+x, 1/2-y, -1/2+z$ )	3.566	3.517	3.438	7.63
Cg2 and Cg3 at ( $1+x, y, z$ )	4.352	3.690	3.488	6.15
Cg3 and Cg2 at ( $-1+x, y, z$ )	4.352	3.488	3.690	6.15

prevented by many short repulsive interactions between fluorine atoms of adjacent molecules. These range from 2.784 to 2.927 Å. The molecular packing of OXA 4 is shown in Fig. 5.

### 3.2. Bulk behavior—equation of state

The thermodynamic state of a solid is defined by pressure  $p$ , temperature  $T$ , and volume  $V$  and described by an appropriate equation of state (see for instance [37,38]). For the interpretation of experimental results for complex substances several semiempirical equations have been developed. These equations have been proven to be more successful for this task compared to equations derived from first principles. The most convenient EOS are such equations that contain parameters that immediately may be obtained from the experiments. For instance the isothermal Murnaghan EOS is usually applied for the

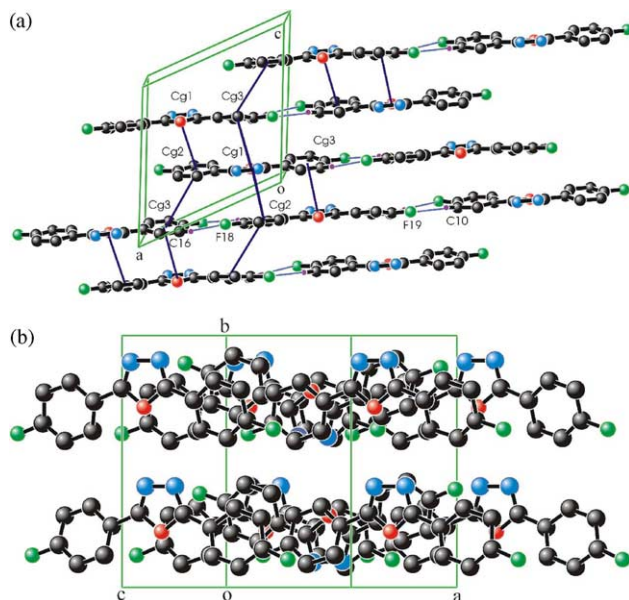


Fig. 2. (a) Stack interactions in the crystal structure of OXA 1 given by the distances between the ring centroids. Additionally the hydrogen bonds are indicated in the molecular layers. (b) Molecular packing in the crystal structure of OXA 1.

Table 4  
 $\pi$ - $\pi$  interactions in OXA 2

Interactions between	DC (Å)	DP (Å)	DP (Å)	$\alpha$ (°)
Cg1 and Cg2 at (1+x, y, z)	4.083	3.438	3.534	4.08
Cg2 and Cg1 at (-1+x, y, z)	4.083	3.534	3.438	4.08
Cg1 and Cg1 at (1+x, y, z)	3.976	3.468	3.468	0.0
Cg2 and Cg2 at (1+x, y, z)	3.976	3.509	3.509	0.0
Cg3 and Cg3 at (1+x, y, z)	3.976	3.560	3.560	0.0

interpretation of experimental data:

$$p = \frac{K_o}{K'_o} \left[ \left( \frac{V_o}{V} \right)^{K'_o} - 1 \right] \quad (1)$$

The index 'o' refers to the initial state at zero pressure.  $K_o$  is the bulk modulus and  $K'_o$  its pressure derivative, i.e.

$$K_o = - \left( \frac{dp}{d \ln V} \right)_{p=0} \quad (2)$$

and

$$K'_o = \left( \frac{dk}{dp} \right)_{p=0} \quad (3)$$

The Murnaghan EOS delivers results for bulk modulus  $K_o$  and its pressure derivative  $K'_o$  with reasonable precision [37]. Measurements in a relatively small pressure range are thus sufficient for the extrapolation of the EOS to higher pressure regions [39] and the equation yields correct moduli for small compressions [40]. A fit to this equation also delivers a value for  $V_o$ , the volume at ambient pressure.

This is used as a quality measure for the whole fit procedure since it can be compared to the value determined by single crystal analysis.

Figs. 6(a) and (b) and Table 5 present the results for the investigated oxadiazole compounds. Some previous results for different aromatic compounds from literature [18,20,21] are supplementary added. From the volume data, it is difficult to decide how the individual compression behavior is influenced by the molecular and supramolecular structure. It is obvious that it is rather similar for these substances despite of their individual molecular and crystal structures. The substitution of fluorine in *para*- and *ortho*-positions of the phenyl ring (OXA 1 and OXA 3) seems to have no significant influence on the compression.

For the meta- and per-fluorinated compounds some deviations occur at increased pressures. In the medium pressure region around 2 GPa a new diffraction line originates and variations of other features are observed in the diffractograms (cf. Fig. 7) leading to the assumption of a structural phase transition. Other severe indications for a transition are derived from larger deviations between the fit of the experimental pattern and the calculated one for OXA 2. Some fitted reflections deviate remarkably from the experimental pattern resulting in a decreasing fit quality. Therefore it has to be assumed, that the initial structure does no longer correctly describe the actual crystal lattice of OXA 2 under pressure and a structural phase transition occurs in the pressure region around 2 GPa. The interpretation of the diffraction data with the old structure is misleading after a phase transition. These changes are fully reversible upon pressure release, the initial structure is fully recovered.

Unfortunately, the quality of the energy dispersive powder diffractograms is not sufficient to perform a structure determination for the new phase. Since no

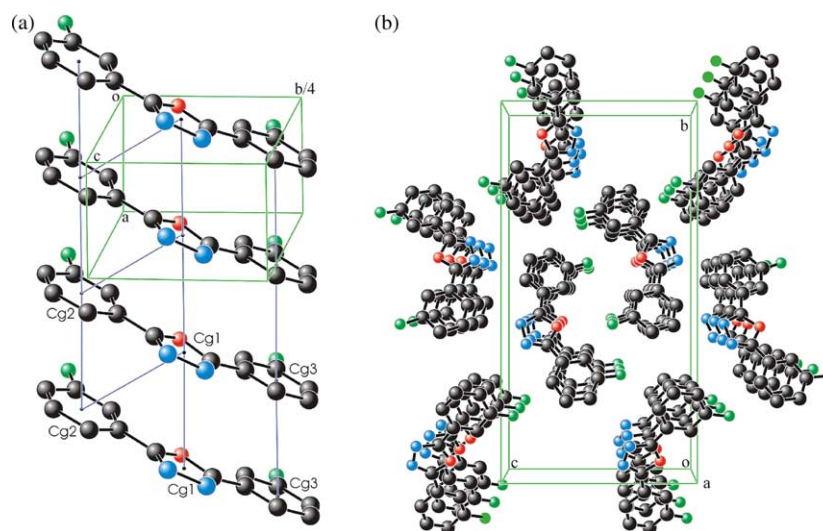


Fig. 3. (a) Stack interactions in the crystal structure of OXA 2 given by the distances between the ring centroids. (b) Molecular packing in the crystal structure of OXA 2.

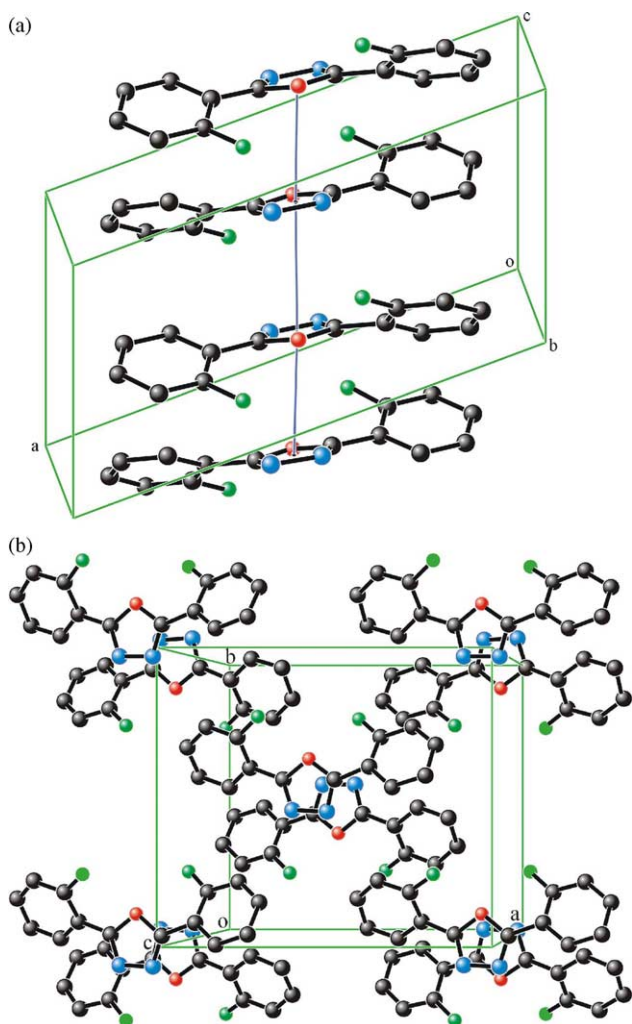


Fig. 4. (a) Stack interactions in the crystal structure of OXA 3. (b) Molecular packing in OXA 3.

assumptions about the possible high-pressure structure could be made an evaluation of the diffractograms is impossible up to now for pressures above 2 GPa. Additional molecular modeling considerations would be necessary to obtain more insight into the possible structural changes and mechanisms.

In the pressure range below 2 GPa the behavior of the initial OXA 2 phase is quite similar to the other fluorine compounds, the EOS parameters are in the same range as for the other compounds. It has to be stated that the fit quality for this compound is generally lower than for the other three samples. Slightly larger errors occur as seen from the volume  $V_0$  as a measure of the fit quality, showing only fair agreement with the value determined from single crystal X-ray investigations.

Also the per-fluorine compound OXA 4 deviates at pressures above 2.0 GPa from the general trend. Again it cannot be ruled out that a phase transition occurs at higher pressures above 2.5 GPa to prevent very close fluorine–fluorine contacts. Then the molecules could be slightly rearranged to avoid too close contacts. However, as

mentioned above, the motions may only be small so that they do not mark sufficiently in the diffractograms. In addition, in this case additional experiments have to be carried out in the future. The rather large  $K'_0$  value not observed for the other oxadiazole compounds could also be an indication for a phase transition.

In general, besides small differences all fluorine compounds investigated here show a rather consistent high-pressure behavior, for those showing a phase transition at least in the pressure region below this transformation. Independent on their structure these compounds do not differ strongly from each other in their  $V$ – $p$  relationship. This also confirms observations of other molecular crystals as for instance of paracetamol [7], were two polymorphs with substantial structural differences have the same bulk compressibility. Only the lattice strain shows characteristic differences due to the different structural arrangement. The EOS parameters are in the range that is typical for organic molecular compounds. These characterize the materials as rather soft and well compressible (cf., for instance [5,8]). This bulk behavior is also observed for such different aromatic compounds like halogenated benzene, benzophenone [18], paracetamol, or phenacetine [6,7,19] as well as for different oligophenylenes [12–14] or other investigated di(phenyl)-1,3,4-oxadiazole crystals [20–22]. Nevertheless, the molecular as well as the supramolecular structure, i.e. the structure of the aromatic system and the packing motif and therefore the different  $\pi$ – $\pi$  and van der Waals interactions between the individual molecules have a small but distinct influence on the compressional behavior.

While the consideration of the bulk properties delivers important elastic parameters describing the pressure response of the solid the description of the lattice distortion in terms of the volume alone is just insufficient to discuss the anisotropy of the compression and therefore the different intermolecular interactions in the crystal. To get some more insight the behavior of the individual unit cell parameters has to be discussed together with the structural features of the compound.

### 3.3. Lattice parameters at high pressures

The compression behavior of one polymorphic form of the unsubstituted 2,5-di(phenyl)-1,3,4-oxadiazole crystal (DPO) was described in [20]. Molecular stacks are formed in a-direction and the  $\pi$ – $\pi$  interactions along these stacks prevent a large compression in this direction. Due to weak van der Waals interactions between adjacent stacks, both other axes show a larger compressibility. This is in accordance with observations on paracetamol and phenacetine [6,7,19] where it was concluded that the greatest compression occurs in such directions where the molecules are only linked by van der Waals forces. Molecular stacks give rise to a pronounced anisotropy of structural strain as observed for instance, in *p*-benzoquinone [6]. The compression behavior in directions with hydrogen bonds

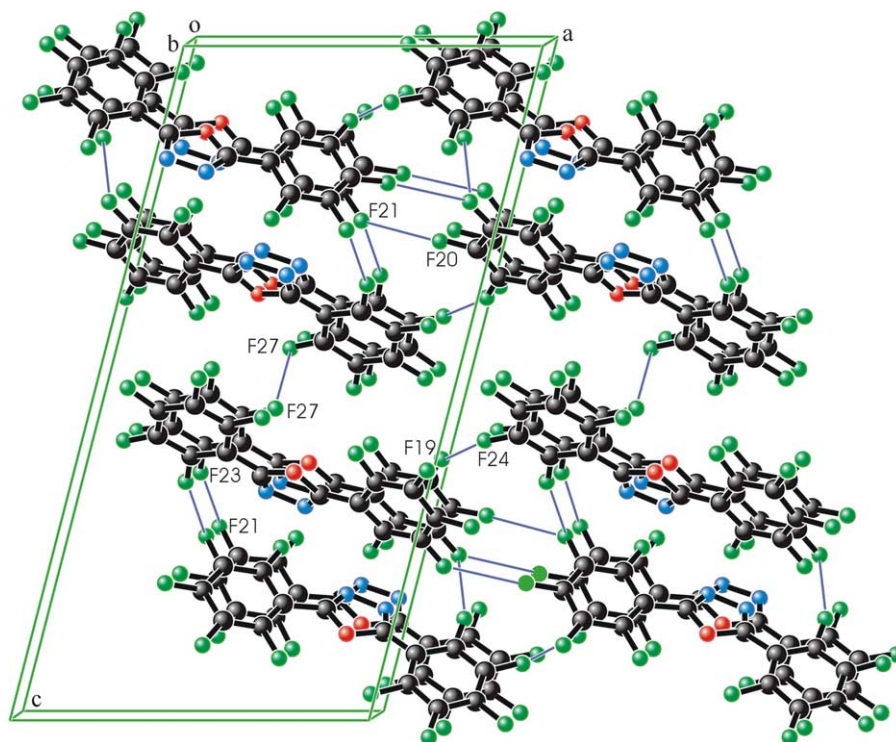


Fig. 5. Molecular packing in OXA 4.

depends on the specific molecular arrangement and therefore also on interactions with the other forces.

The crystal structure changes remarkably if the terminal hydrogen atom of DPO is substituted by a fluorine atom (OXA 1). Here, a layered arrangement is observed in the *a,c*-plane together with hydrogen bonds in that layer. The compression of the unit cell is illustrated in Fig. 8(a). Only one axis—the *c*-axis—is well compressible (approximately 15% up to 5 GPa), the remaining two axes are less compressible. They diminish in the pressure range up to 5 GPa only by 6–7%. The small compressibility of the *a*-axis is explained by the strength of the  $\pi$ – $\pi$  interactions

between oxadiazole (acceptor) and phenyl (donor) rings of adjacent molecules (cf. Fig. 2(a)). Additionally, the two intermolecular hydrogen bonds between C–H and fluorine in the *a,b*-plane contribute to the low compressibility in these directions and therefore also stabilize the structure.

Fig. 8(b) presents results for the *ortho*-compound OXA 3. The OXA 3 molecules show a larger deviation from planarity compared to many other investigated di(phenyl)-1,3,4-oxadiazoles [20–22,34,41]. They show a larger torsion of the phenyl ring around the interring bond in opposite directions for both rings (approximately  $\pm 29^\circ$ ). Both phenyl-fluorine bonds point to the oxygen atom of the

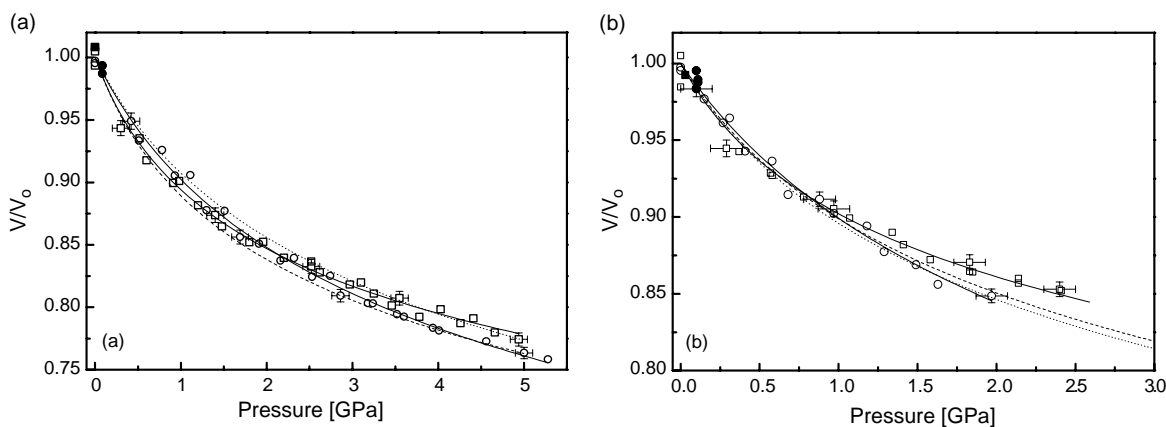


Fig. 6. Equation of state for (a): OXA 1 [○] and OXA 3 [□] and (b): OXA 2 [○] and OXA 4 [□]. Full symbols represent data after pressure release. Reference data from 2,5-di(phenyl)-1,3,4-oxadiazole (dotted line) [20], and diphenyl (dashed line) [18] are added for comparison to (a) and data for 2,5-bis(4-diaminophenyl)-1,3,4-oxadiazole (dotted line) [21] and terphenyl (dashed line) [18] to (b).

Table 5

EOS parameters for OXA1–OXA4 together with some values for other 2,5-di(phenyl)-1,3,4-oxadiazoles and other aromatic compounds for comparison from literature

Compound	$V_0$ (structure determination) ( $\text{\AA}^3$ )	$V_0$ (EOS—Eq. (1)) ( $\text{\AA}^3$ )	$K_0$ (GPa)	$K'_0$
OXA 1	1151.259	$1156.2 \pm 2.7$	$6.9 \pm 0.8$	$6.2 \pm 0.3$
OXA 2	1199.276	$1182.3 \pm 3.0$	$6.6 \pm 2.3$	$6.3 \pm 1.2$
OXA 3	1141.316	$1143.6 \pm 2.7$	$5.1 \pm 0.6$	$9.1 \pm 0.4$
OXA 4	1323.496	$1323.3 \pm 2.3$	$5.2 \pm 0.6$	$11.2 \pm 0.5$
DPO [20]	1148.307	1147.8	7.3	6.7
DAPO [21]	2457.033	2460.3	5.6	8.2
Diphenyl [18] <sup>#</sup>			5.1	8.1
Terphenyl [18] <sup>#</sup>			5.8	8.4

<sup>#</sup>: Values calculated from pressure-volume data. (DPO—2,5-di(phenyl)-1,3,4-oxadiazole, monoclinic structure, space group  $P2_1/c$ ; DAPO—2,5-bis(4-aminophenyl)-1,3,4-oxadiazole, orthorhombic structure, space group  $Pbca$ )

oxadiazole ring but due to the ring torsion they are above and below the molecular plane. The molecules are arranged in layers in the  $a,b$ -plane. Molecular stacks with opposed molecules (given by the direction of the connection between the center of the oxadiazole ring and the oxygen atom) are arranged in  $c$ -direction so that the overlap of the  $\pi$ -systems is rather weak and only given by the oxadiazole ring (Fig. 4(a)). This is the reason for the large compressibility of the axis perpendicular to the molecular planes where also a possible planarization of the molecules could deliver additional contributions. In  $a$ -direction, stronger interactions of the fluorine atoms with carbon atoms of adjacent phenyl rings and therefore the formation of hydrogen bonds contribute to the very low compression in the range up to 5 GPa. The weak  $\pi$ - $\pi$  interactions due to the overlap of only the oxadiazole rings and the less important components of the fluorine interactions in  $b$ -direction allows a good compressibility of this unit cell axis.

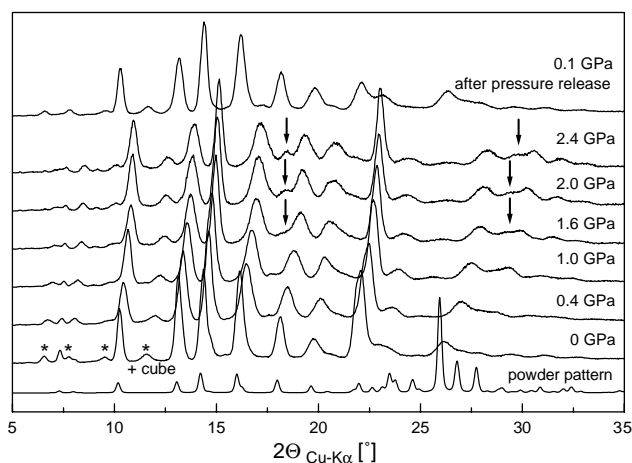


Fig. 7. X-ray diffractograms of OXA 2 under increasing pressure. Indications for a structural transition are marked by arrows, the asterisks denote escape peaks from the detector. Small influences of the gasketing cube may contribute to line broadening in the range  $16$ – $22^\circ$  ( $2\theta_{Cu-K\alpha}$ ).

The axes of OXA 2 exhibit a rather analogous compressional behavior below 2 GPa as Fig. 8(c) summarizes. The compressibility of the  $a$ -axis is slightly higher compared to that of the  $b$ - and  $c$ -axes. In general, the compressibility is in the range of the less compressible axes of the other investigated compounds. OXA 2 is characterized by stacks in  $a$ -direction. Again, the molecular planes are inclined against the stack axis, therefore the  $\pi$ - $\pi$  interactions are oriented on a diagonal of the  $a,b$ -plane, explaining the nearly identical behavior of both axes.

Results for the perfluorinated compound OXA 4 below 2 GPa are given in Fig. 8(d). Interestingly, with approximately  $14^\circ$  the torsion angles between phenyl and oxadiazole rings are in the same range as those of OXA 1 (cf. Table 2). Both phenyl rings are rotated in the same direction out of the molecular plane. The structure is characterized by the arrangement of parallel molecules in  $b$ -direction but due to the large intermolecular distance no overlap between the  $\pi$  systems appears and therefore  $\pi$ - $\pi$  interactions are missing. However, a network of fluorine–fluorine interactions evolves preferentially in the  $a,c$ -plane between neighbored molecules with usual distances around  $2.79$ – $2.93$   $\text{\AA}$ . Compared to the other investigated compounds the axes show a decreased compressibility. The low compressibility of the  $a$ -axis is attributed to the fluorine–fluorine interactions. The compressibility of the  $b$ - and  $c$ -axes of approximately 5% up to a pressure of 2 GPa corresponds to intermediate values compared to the other compounds. This has also to be ascribed to the fluorine interactions since the intermolecular  $\pi$ -interactions are not as strong as observed in the perfect stack arrangement of other oxadiazole compounds, for instance in DPO [20].

The anisotropy of the compression in the different compounds is reflected by the anisotropy of strain. The corresponding strain tensors may be obtained from the measured changes of the cell parameters under pressure to obtain additional information on the most and least compressible directions in the structures. Therefore, Table 6 is included with selected values of the cell parameters as function of pressure for all four oxadiazole compounds, so that the strain tensors may be calculated, for instance using the program Strain [42].

All compounds under investigation were also studied after full pressure release still within the high-pressure setup. In every case, a full reversibility of the compression was found. Neither enduring modifications nor irreversible changes in the structure could be detected. The determined unit cell parameters were well in the range of the initial values taking into account reasonable error limits as for instance slight stress in the sample and epoxy cube that were accumulated during the pressure run and vanished completely only after dismounting the sample off the press.

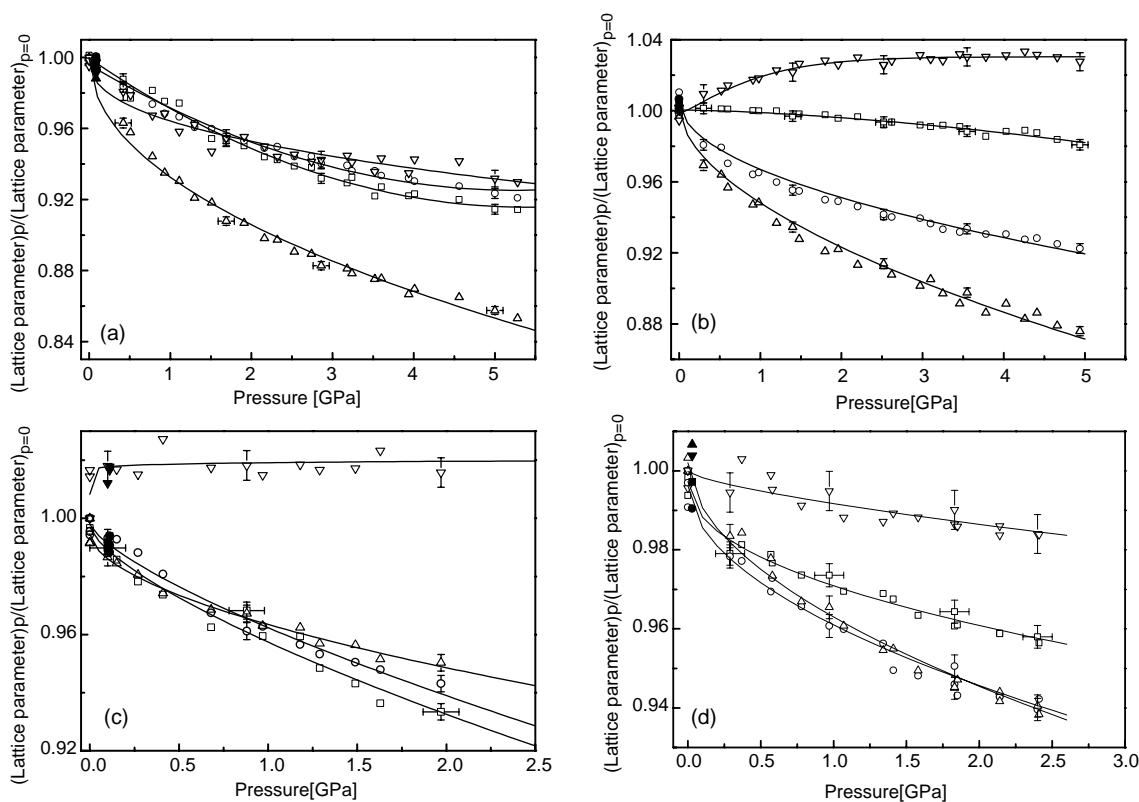


Fig. 8. Anisotropic pressure response of the crystal lattice for OXA 1 (a), OXA 3 (b), OXA 2 (c), and OXA 4 (d). (□  $a/a_0$ ; ○  $b/b_0$ ; △  $c/c_0$ ; ▽  $\beta/\beta_0$ ; full symbols represent data after pressure release).

#### 4. Concluding remarks

As demonstrated here for the example of different fluorine 2,5-di(phenyl)-1,3,4-oxadiazoles the variation of the substitution scheme changes the molecular configuration and the conformation due to varied intramolecular interactions. While the main intermolecular forces are the same ( $\pi$ - $\pi$  interactions between the  $\pi$ -systems of the oxadiazole and phenyl rings and van der Waals forces) a different crystal structure results with modified packing motifs from the different three-dimensional network of these intermolecular forces that evolves for the differently substituted molecules. Nevertheless, some motifs like that for the  $\pi$ - $\pi$  interactions (nearly parallel and interacting oxadiazole and phenyl rings) may resemble each other. This results in a specific anisotropic pressure response of the crystal lattice. While the EOS parameters are nearly the same for all investigated compounds the compounds differ in their individual behavior of the lattice parameters with pressure. For stack-like arrangements this behavior is fairly well determined by the orientation of the molecular planes against the stack and the unit cell axes and the evolving strong  $\pi$ - $\pi$  interactions within the stack as well as by the van der Waals forces between different stacks. In structures lacking such unambiguous features and showing a more complex pattern, contributions of various interactions have to be considered in the different unit cell directions.

Additional support may be obtained by further investigations for instance applying improved X-ray methods or by studying the anisotropy of the compression using the strain tensor as carried out for instance in [6,7,19]. Also molecular modeling and theoretical considerations seriously contribute to a better description of the high-pressure behavior of such aromatic systems.

Table 6  
Cell parameters at selected pressures for compounds OXA1–OXA4

	$p$ (GPa)	$a$ (Å)	$b$ (Å)	$c$ (Å)	$\alpha$ (°)
OXA 1	0.9	10.19	11.08	10.05	112.65
	1.9	9.92	10.91	9.74	111.12
	3.5	9.63	10.71	9.41	108.84
	4.6	9.61	10.61	9.30	109.53
	5.0	9.55	10.57	9.22	108.38
OXA 2	0.7	3.83	23.45	12.05	91.69
	1.3	3.77	23.10	11.91	91.63
	2.0	3.71	22.86	11.83	91.54
OXA 3	1.0	13.86	11.97	6.71	112.30
	2.0	13.80	11.76	6.53	113.15
	3.1	13.74	11.61	6.41	113.49
	4.0	13.70	11.54	6.31	113.74
	4.9	13.60	11.44	6.20	113.33
OXA 4	0.6	12.03	4.57	23.03	104.47
	1.0	11.99	4.52	22.84	104.43
	1.6	11.87	4.46	22.46	103.73
	2.4	11.80	4.42	22.25	103.29

## Acknowledgements

The authors thank Ch. Lathe and the GeoForschungs-Zentrum Potsdam for the possibility of using the MAX-80 equipment and the support.

This work was supported in parts by Deutsche Forschungsgemeinschaft under Grant Schu 842/12-3 and Ministerium für Wissenschaft, Forschung und Kultur des Landes Brandenburg under Grant HWP 24#2597-04/328.

## References

- [1] J.V. Badding, *Ann. Rev. Mater. Sci.* 28 (1998) 631.
- [2] J.V. Badding, L.J. Parker, D.C. Nesting, *J. Solid State Chem.* 117 (1995) 229.
- [3] R.J. Hemley, N.W. Ashcroft, *Phys. Today* 51 (1998) 26.
- [4] A. Katrusiak, P. McMillan (Eds.), *High-Pressure Crystallography NATO Science Series II: Mathematics, Physics and Chemistry* vol. 140, Kluwer, Dordrecht, 2004.
- [5] R.J. Hemley, P. Dera, *Rev. Mineral. Geochem.* 41 (2000) 335.
- [6] E.V. Boldyreva, *Cryst. Eng.* 6 (2004) 235.
- [7] E.V. Boldyreva, *J. Mol. Struct.* 647 (2003) 159.
- [8] A. Katrusiak, *Cryst. Res. Technol.* 26 (1991) 523.
- [9] R.S. Payne, R.J. Roberts, R.C. Rowe, M. McPartlin, A. Bashal, *Int. J. Pharm.* 145 (1996) 165.
- [10] R.J. Roberts, R.S. Payne, R.C. Rowe, *Eur. J. Pharm. Sci.* 9 (2000) 277.
- [11] P. Puschnig, C. Ambrosch-Draxl, G. Heimel, E. Zojer, R. Resel, G. Leising, M. Kriechbaum, W. Graupner, *Synth. Met.* 116 (2001) 327.
- [12] G. Heimel, Q. Cai, C. Martin, P. Puschnig, S. Guha, W. Graupner, C. Ambrosch-Draxl, M. Chandrasekhar, G. Leising, *Synth. Met.* 119 (2001) 371.
- [13] S. Guha, W. Graupner, R. Resel, M. Chandrasekhar, H.R. Chandrasekhar, R. Glaser, G. Leising, *Synth. Met.* 101 (1999) 180.
- [14] P. Puschnig, K. Hummer, C. Ambrosch-Draxl, G. Heimel, M. Oehzelt, R. Resel, *Phys. Rev. B* 67 (2003) 235321.
- [15] A. Brillante, R.G. Della Valle, C. Ulrich, K. Syassen, *J. Chem. Phys.* 107 (1997) 4628.
- [16] A. Brillante, R.G. Della Valle, C. Polizzi, K. Syassen, *Physica B* 265 (1999) 199.
- [17] M. Oehzelt, G. Heimel, R. Resel, P. Puschnig, K. Hummer, C. Ambrosch-Draxl, K. Takemura, A. Nakayama, *J. Chem. Phys.* 119 (2003) 1078.
- [18] Landolt-Börnstein, in: K. Schäfer (Ed.), *Zahlenwerte und Funktionen aus Naturwissenschaften und Technik Neue Serie, Gruppe IV, Band 4: Eigenschaften der Materie bei hohen Drücken*, Springer, Berlin, 1980.
- [19] T.P. Shakhshneider, E.V. Boldyreva, M.A. Vasilchenko, H. Ahsbahs, H. Uchtmann, *J. Struct. Chem.* 40 (1999) 892.
- [20] O. Franco, G. Reck, I. Orgzall, B. Schulz, *J. Phys. Chem. Solids* 63 (2002) 1805.
- [21] O. Franco, I. Orgzall, G. Reck, S. Stockhause, B. Schulz, *J. Phys. Chem. Solids*, in press.
- [22] O. Franco, Thesis, Universität Potsdam, Potsdam, 2002.
- [23] I.D.H. Oswald, D.R. Allan, W.D.S. Motherwell, S. Parsons, *Acta Cryst. B* 61 (2005) 69.
- [24] M. Bujak, A. Budzianowski, A. Katrusiak, *Z. Kristall.* 219 (2004) 573.
- [25] Ch.-J. Tsai, Y. Chen, *J. Polym. Sci. Pt. A, Polym. Chem.* 40 (2002) 293.
- [26] M. Golfier, R. Milcent, *Synthesis* 12 (1979) 946.
- [27] A.T. Prudchenko, S.A. Vereshchagina, V.A. Barkhash, N.N. Vorozhtsov Jr., *Zhurnal Obshchei Khimii* 37 (1967) 2195.
- [28] G.M. Sheldrick, *SHELX-97*, Universität Göttingen, 1997.
- [29] O. Shimomura, S. Yamaoka, T. Yagi, M. Wakatsuki, K. Tsuji, H. Kawamura, N. Hamaya, O. Fukunaga, K. Aoki, S. Akimoto, in: S. Minomura (Ed.), *Solid State Physics under Pressure*, D. Reidel, Dordrecht, 1985, p. 351.
- [30] J. Shen, J.B. Parise, R. Li, D.J. Weidner, V. Vaughan, in: M.H. Manghni, T. Yagi (Eds.), *Properties of Earth and Planetary Materials at High Pressure and Temperature Geophysical Monograph Series* vol. 101, American Geophysical Union, Washington, DC, 1998, p. 139.
- [31] D.L. Decker, *J. Appl. Phys.* 42 (1971) 3239.
- [32] J.M. Brown, *J. Appl. Phys.* 86 (1999) 5801.
- [33] W. Kraus, G. Nolze, *Powder Cell* 2.3, Bundesanstalt für Materialforschung und-prüfung (BAM), Berlin, 1999.
- [34] G. Reck, private communication, to be published.
- [35] X. Zheng, Z. Li, Y. Wang, W. Chen, Q. Huang, C. Liu, G. Song, *J. Fluorine Chem.* 123 (2003) 163.
- [36] A.L. Spek, *Platon. A Multipurpose Crystallographic Tool*, Utrecht University, Utrecht, 2003.
- [37] C.S. Menoni, I.L. Spain, *High Pressure Measurement Techniques* in: G.N. Peggs (Ed.), Applied Science Publishers, London, 1983, p. 125.
- [38] J.-P. Poirier, *Introduction to the Physics of the Earth's Interior*, second ed., Cambridge University Press, Cambridge, 2000.
- [39] O. Anderson, *Phys. Earth Planet. Inter.* 1 (1968) 169.
- [40] R.J. Angel, in: R.M. Hazen, R.T. Downs (Eds.), *High-Pressure, High-temperature Crystal Chemistry Rev. Mineral. Geochem.* vol. 41 (2001), p. 35.
- [41] S. Stockhause, M.S. Wickleder, G. Meyer, I. Orgzall, B. Schulz, *J. Mol. Struct.* 561 (2001) 175.
- [42] Y. Ohashi, in: R.M. Hazen, L.W. Finger (Eds.), *Comparative Crystal Chemistry*, Wiley, New York, 1982.